



# DISASTER RISK PROFILE PEOPLE'S REPUBLIC OF CHINA

**Inner Mongolia Autonomous Region and Xinjiang  
Uygur Autonomous Region**

TA-9878 REG: Developing a Disaster Risk Transfer  
Facility in the Central Asia Regional Economic  
Cooperation (CAREC) Region

**March 2022**



About this document

TA-9878 REG: Developing a Disaster Risk Transfer Facility in the Central Asia Regional Economic Cooperation Region aims at developing regional disaster risk financing solutions for CAREC member states. It provides high-level disaster risk profiles for all CAREC member states for earthquake, floods, and infectious disease risk. The TA will then design and pilot a bespoke regional disaster risk transfer facility. This is to support CAREC member states in their management of disaster risk.

The disaster risk profiles collate information on flood, earthquake and infectious disease exposure, hazards, physical and social vulnerability, coping capacity, historical losses and impacts, and risk analysis for all CAREC member states. Much of this information is being collated on a regionally consistent basis for the first time. This includes cutting-edge flood, earthquake, and infectious disease modeling.

The profiles are logically structured:

- i. **Risk analysis:** results from risk modeling;
- ii. **Historical losses and impacts:** data collected from national and international databases;
- iii. **Hazard:** physical processes which cause floods, earthquakes and infectious disease outbreaks;
- iv. **Exposure:** characteristics of livelihoods and economic value at risk and;
- v. **Vulnerability:** socio-economic vulnerability and coping capacity;

These profiles are accompanied by a separate technical note which details the data and methodologies used, and discusses appropriate limitations.

Contents

Profile Summary	8
Chapter 1: Risk analysis	12
Chapter 2: Historical losses and impacts	26
Chapter 3: Hazard	28
Chapter 4: Exposure	38
Chapter 5: Vulnerability	42





# List of abbreviations

AAL	Average Annual Loss
AALR	Average Annual Loss Ratio
ADB	Asian Development Bank
ADM	Administrative Boundary
AAPA	Average Annual Number of People Affected
CAREC	Central Asia Regional Economic Cooperation
COVID-19	Coronavirus disease
CCHF	Crimean-Congo Hemorrhagic Fever
DRF	Disaster Risk Financing
EP	Exceedance Probability
EMS	Emergency Management System
GEM	Global Earthquake Model Foundation
IPCC	Intergovernmental Panel on Climate Change
IDPs	Internally displaced persons
JBA	Jeremy Benn Associates
RCP	Representative Concentration Pathway
TA	Technical Assistance

## Currency

Currency Unit	United States Dollar/s (\$)
---------------	-----------------------------

# List of figures and tables

Figure 1	Breakdown of average annual loss and loss ratio by autonomous regions - earthquake	12
Figure 2	Average annual loss by asset types - earthquakes	13
Figure 3	Breakdown of average annual fatalities by region - earthquake	13
Figure 4	Breakdown of average annual number of people affected by region - earthquake	14
Figure 5	Exceedance probability curves IMAR - Earthquakes	14
Figure 6	Exceedance probability curves XUAR - Earthquakes	16
Figure 7	Breakdown of average annual loss and loss ratio by region - flood	18
Figure 8	Breakdown of average annual fatalities by region - flood	19
Figure 9	Breakdown of average annual number of people affected by region - flood	19
Figure 10	Exceedance probability curves - floods - IMAR	20
Figure 11	Exceedance probability curves - floods - XUAR	21
Figure 12	Exceedance probability curves - pandemic, including CCHF, Nipah virus infection, respiratory viruses and combined (all pathogens) - IMAR	22
Figure 13	Exceedance probability curves - pandemic, including CCHF, Nipah virus infection, respiratory viruses and combined (all pathogens) - XUAR	24
Figure 14	Map of surface water (pluvial) flooding (areas in purple) at the 200-year return period level for the Baotou region	31
Figure 15	Map of surface water (pluvial) flooding (areas in purple) at the 200-year return period level for the Urumqi region	32
Figure 16	Breakdown of building types - PRC	40



Table 1	Average annual losses – pandemic, including CCHF, Nipah virus infection, respiratory viruses and combined (all pathogens)	24
Table 2	Total impacts from floods and earthquakes, 1990-2019	26
Table 3	The most impactful flood and earthquake events, 1900 – 2019	27
Table 4	Notable infectious disease outbreaks, 1990-2021	27
Table 5	Baotou 24-hr duration extreme precipitation intensity (mm/hr)	36
Table 6	Urumqi 24-hr duration extreme precipitation intensity (mm/hr)	37
Table 7	Population totals, distribution and trends	38
Table 8	Key economic indicators	39
Table 9	Socio-economic vulnerability indicators	42
Table 10	Key coping capacity indicators	42
Table 11	Key Protection Gap indicators – IMAR	44
Table 12	Key Protection Gap indicators – XUAR	44





# Profile Summary

**The People’s Republic of China (the PRC) spreads over a vastly diverse geographical area of 9.6 million square kilometers, and is home to approaching 1.4 billion people, the world most populous country.**

It shares borders with Mongolia, the Russian Federation, North Korea, Viet nam, Lao People’s Democratic Republic, Myanmar, India, Bhutan, Nepal, Pakistan, Afghanistan, Tajikistan, Kyrgyz Republic, and Kazakhstan. The Yellow, East China, and South China seas lie to the east. The Himalayan, Karakoram, and Altai mountain ranges separate the PRC from its neighbors to the west.

The Qinghai-Tibet Plateau in the southwest is a cold, mountainous region. The northwest is a highland with large desert basins. The east holds almost all of the PRC’s lowlands. Among the PRC’s major rivers are the Changjiang (Yangtze), Huanghe (Yellow River) and Zhujiang (Pearl River).



The risk profile for the PRC refers to the two autonomous regions that are part of the Central Asian Regional Economic Cooperation (CAREC): Inner Mongolia Autonomous Region (IMAR) and Xinjiang Uygur Autonomous Region (XUAR). XUAR occupies the northwestern corner of the PRC, bordered by the Qinghai and Gansu autonomous regions to the east, the Tibet Autonomous Region to the south, Afghanistan to the southwest, Kyrgyz Republic and Tajikistan to the west, Kazakhstan to the northwest, the Russian Federation to the north, and Mongolia to the northeast. The IMAR is a vast stretch of land across the northern PRC, bordered by Mongolia and the Russian Federation in the north.

XUAR has a wide and varied landscape split across 5 main regions: the Northern Highlands, the Junggar (Dzungarian) Basin, the Tian Shan mountains, the Tarim Basin, and the Kunlun Mountains. IMAR is essentially an inland plateau with a flat surface lying at an elevation of about 3,300 feet above sea level and fringed by mountains and valleys. Its southern boundary is formed by a series of high ridges with an average height of between 4,500 and 6,000 feet. To the northwest the land falls away toward the centre of the Gobi desert. The Huang He (Yellow River) loops in a northward then southward direction through south-central IMAR, providing irrigation water for the area.



Both XUAR and IMAR experience common disaster events as shown in Box 1a and Box1b respectively. Average annual loss (AAL) due to earthquakes in XUAR is modeled at over \$280m while the average annual number of people affected, and number of fatalities is 87,044 and 84 respectively. For IMAR, the numbers are lower with an AAL of \$120m and average annual number of people affected 41,290. The loss from a 100-year earthquake event is modeled at around \$2.2billion in IMAR and \$2.9 billion in XUAR.

**A LOW FREQUENCY, HIGH IMPACT EARTHQUAKE (1-IN-100-YEAR) COULD CAUSE OVER \$2 BILLION OF LOSS IN BOTH REGIONS.**

Box 1a: IMAR Profile Summary

<div>  <b>GDP: \$279,000,000,000 (2020)</b> </div>		<div>  <b>Population: 24,700,000 (2010)</b> </div>	
1 IN 100 YEAR FLOOD ECONOMIC LOSS	1 IN 100 YEAR EARTHQUAKE LOSS	AVERAGE ANNUAL LOSS FLOOD	AVERAGE ANNUAL LOSS EARTHQUAKE
\$1,500,000,000	\$2,200,000,000	\$247,700,000	\$121,600,000
AVERAGE ANNUAL PEOPLE AFFECTED FLOOD	AVERAGE ANNUAL PEOPLE AFFECTED EARTHQUAKE	AVERAGE ANNUAL PEOPLE AFFECTED INFECTIOUS DISEASE	
162,809	41,290	275,707	

Box 1b: XUAR Profile Summary

<div>  <b>GDP: \$211,000,000,000 (2019)</b> </div>		<div>  <b>Population: 21,800,000 (2010)</b> </div>	
1 IN 100 YEAR FLOOD ECONOMIC LOSS	1 IN 100 YEAR EARTHQUAKE LOSS	AVERAGE ANNUAL LOSS FLOOD	AVERAGE ANNUAL LOSS EARTHQUAKE
\$1,200,000,000	\$2,900,000,000	\$106,600,000	\$282,900,000
AVERAGE ANNUAL PEOPLE AFFECTED FLOOD	AVERAGE ANNUAL PEOPLE AFFECTED EARTHQUAKE	AVERAGE ANNUAL PEOPLE AFFECTED INFECTIOUS DISEASE	
104,315	87,044	268,488	



For flood, IMAR has the higher annual risk with the AAL modeled at \$247.7 million. The average annual number of people affected by floods in the region is estimated to be 163,000 with fatalities averaging 8. The loss from a 100-year flood event is modeled at around \$1.5 billion. In XUAR, AAL for flood is expected to be \$106 million with 104,315 people impacted and 5 fatalities.

Exposure to infectious disease outbreaks is similar for IMAR and XUAR with respiratory pathogens accounting for most of the risk. A 1-in-100-year event could see around 275,00 people infected in both regions. In XUAR there is also a low background risk to Crimean-Congo Haemorrhagic Fever.

In the past three decades, floods and earthquakes combined are estimated to have affected over 3.5 million people and resulted in over \$1.1 billion in damage across IMAR and XUAR.

Multiple climate change studies indicate that the East Asian monsoon might become more variable impacting IMAR. Whilst trends in future winter precipitation have some uncertainty, the summer (July to September) mean precipitation could decrease by 10 to 20% for parts of the region.

XUAR’s annual mean precipitation could increase by 10 to 40% over the Kunlun Mountains and the southern borders of the Taklamakan Desert under both RCP4.5 and RCP8.5 by the 2050s. Potential drying between 10 and 20% is seen for sections of the Taklamakan and the drier areas of the Tarim River Basin in the north.

Insurance penetration in both regions is high, non-life insurance penetration is 1.24% in IMAR and 2.66% in XUAR. These high figures are driven by compulsory crop insurance through the China Agricultural Policy Insurance Program (CAPIP). In 2012, 95% of farms in IMAR were insured through this Program, while livestock insurance is also intended to be compulsory.<sup>1</sup> By contrast, buildings insurance for flood and earthquake risk is less extensive, although specific data is difficult to ascertain.



<sup>1</sup> Zhao, Y., Chai, Z., Delgado, M. and Preckel, P. (2016) An empirical analysis of the effect of crop insurance on farmers' income: Results from IIMAR in China. *China Agricultural Economic Review* 8(2): 299-313



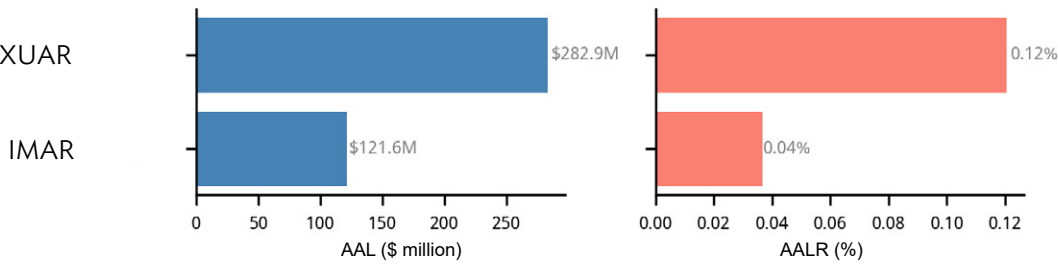
# Risk analysis

The extent and geographic pattern of earthquake, flooding, and infectious disease across IMAR and XUAR are revealed through probabilistic modeling. Such modeling helps illustrate how natural phenomena interact with areas of high concentrations of population and assets to cause economic loss and damage.

## Earthquake Risk

Average annual loss due to earthquakes in the two autonomous regions of the PRC is estimated at \$404.5 million. XUAR has the higher average annual loss (AAL) of the two autonomous regions at \$282.9 million, while IMAR has an AAL of \$121.6 million.

Figure 1: Breakdown of average annual loss and loss ratio by autonomous regions - earthquake



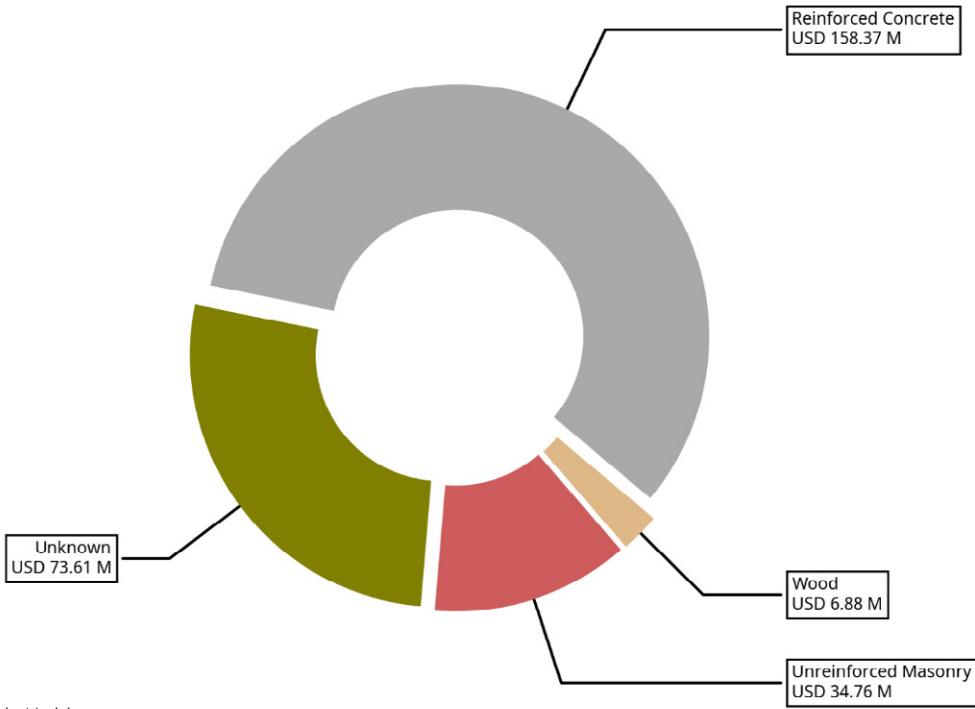
Source: Global Earthquake Model

The average annual loss ratio (AALR) in each autonomous regions is the AAL for the autonomous regions normalized by the total exposed value of buildings in that autonomous regions. The AALR represents the proportion of the replacement value of the building stock that is expected to be lost due to damage. As a normalized risk metric, the AALR enables comparison of the relative risk across the different autonomous regions of the country.

Figure 1 compares the AAL (left) and the AALR (right) for each autonomous regions. AALR is expressed as a percentage of the total replacement value of buildings in the respective autonomous regions. Looking at the relative risk, XUAR is also the autonomous region with the greater AALR.

As seen in Figure 2, reinforced concrete structures contribute the most to the overall average annual loss in economic terms at \$158.4 million, followed by unknown structures with an aggregate AAL of \$73.6 million.

Figure 2: Average annual loss by asset types - earthquakes



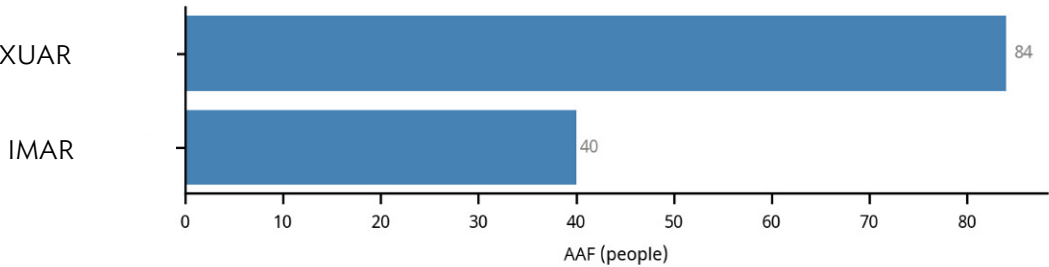
Source: Global Earthquake Model



Average annual fatalities (AAF) due to earthquakes are estimated at 123 in the two autonomous regions of the PRC. XUAR has the higher AAF at 84 while IMAR has 40 (as seen in Figure 3), further emphasizing the higher risk in this region.

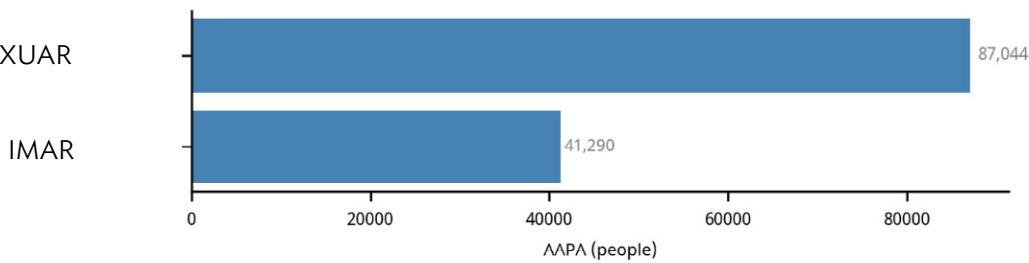
For the purposes of this report, the number of people affected by earthquakes is defined as the population that can be expected to witness earthquake-caused ground shaking of Modified Mercalli Intensity (MMI) VI or higher (corresponding to strong shaking, capable of causing slight damage or higher). As seen in Figure 4, 128,334 people are estimated to be affected by earthquakes on an average annual basis in the two autonomous regions of the PRC. XUAR has the higher average annual number of people affected at 87,044 while IMAR has 41,290.

Figure 3: Average annual fatalities - earthquake



Source: Global Earthquake Model

Figure 4: Average number of people affected - earthquake

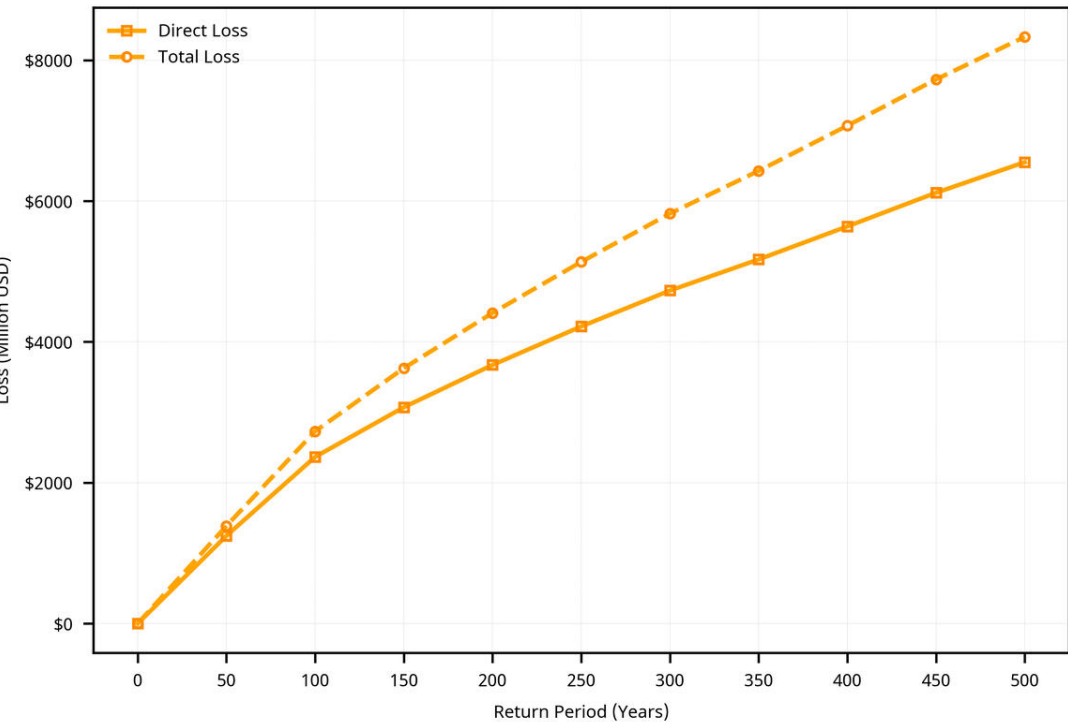


Source: Global Earthquake Model





Figure 5: Exceedance probability curves IMAR – earthquakes

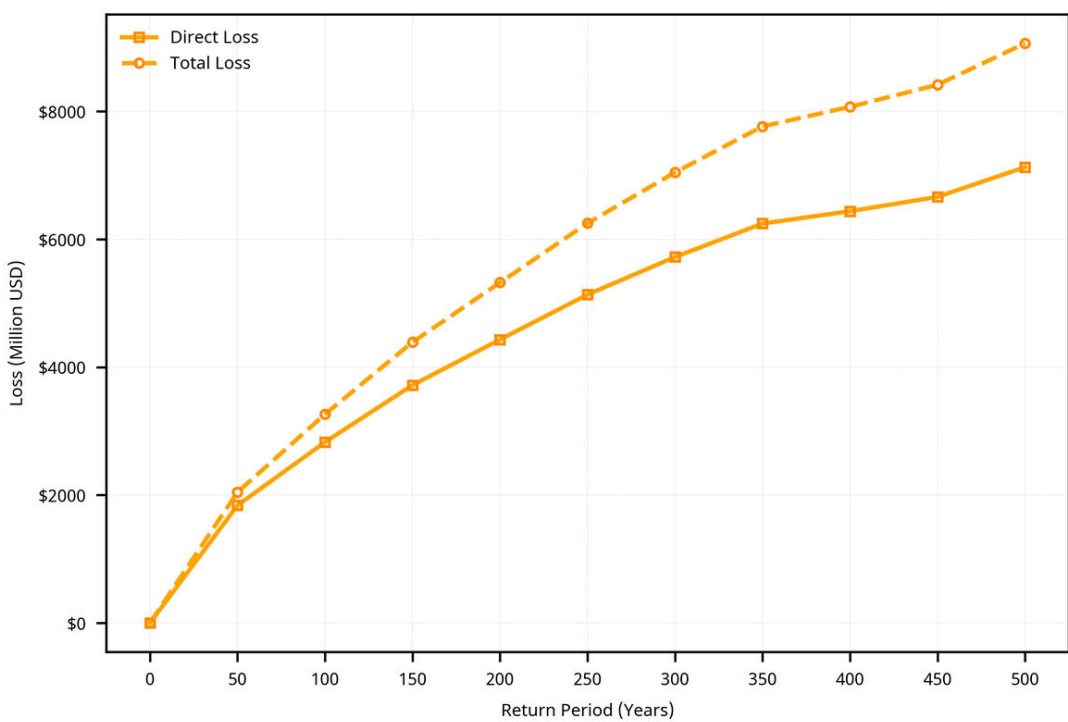


Source: Global Earthquake Model

The exceedance probability (EP) curves for earthquake for IMAR and XUAR are shown in Figure 5 and Figure 6 respectively. The EP curve shows the total loss from all events in any given year. Curves are modeled for both direct and total loss. Direct loss displays the modeled loss to residential, industrial and commercial assets. Total loss accounts for secondary impacts from the onset of disaster events, accounting for the reconstruction time.

In IMAR, direct loss increases from \$2.2 billion at the 100 year return period to over \$6 billion for the 500-year return period. Total loss increases from just under \$1.5 billion at the 50-year return period to more than \$8 billion at the 500-year return period. The curve increases steadily as events become more severe.

Figure 6: Exceedance probability curves XUAR – earthquakes



Source: Global Earthquake Model

In XUAR, the EP curve increases at a faster rate, illustrating the higher risk. Between the 50-year and 500-year return period total loss increases more quickly than direct loss. Direct loss is modeled at \$2.9 billion for the 100-year event, rising to over \$6.5 billion for the 500-year event.

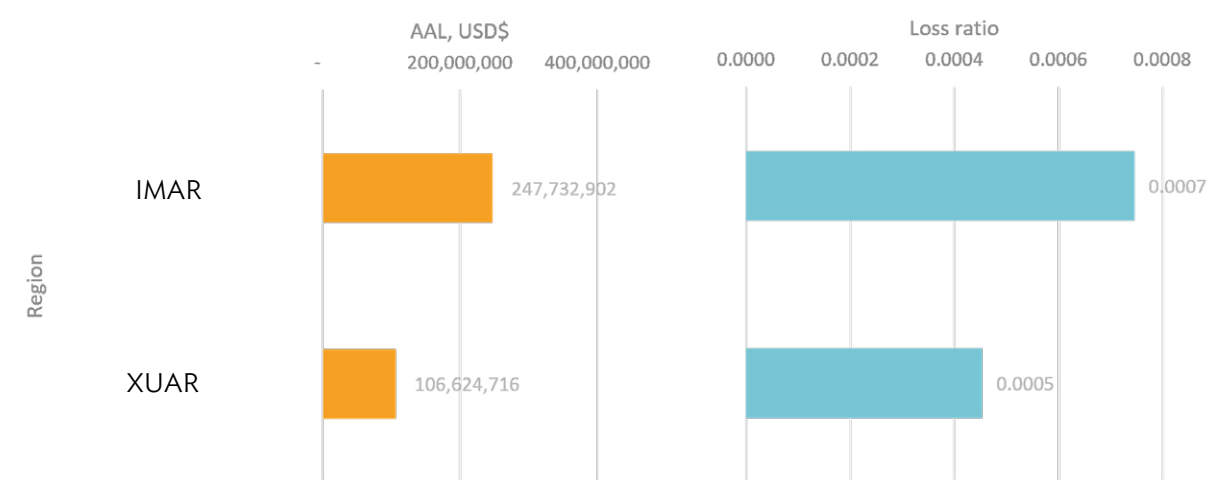


Flood Risk

Flood loss differs materially between the two regions. The average annual loss is \$247.7 million in IMAR and \$106.6 million in XUAR.

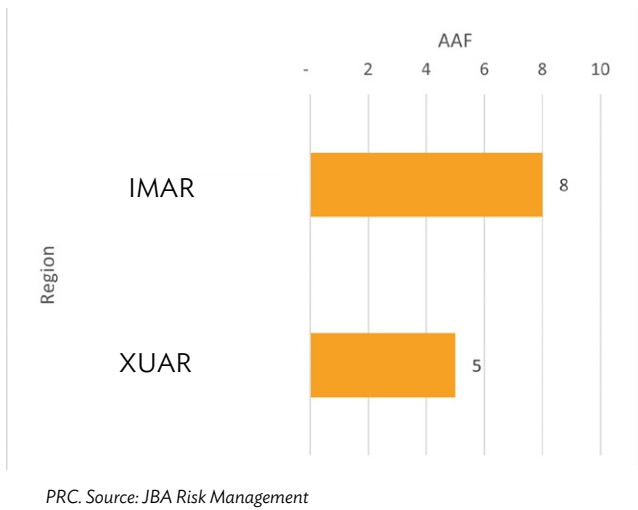
Figure 7 shows the average annual loss ratio in IMAR and XUAR. The distribution and density of people and assets in IMAR is more concentrated, increasing vulnerability to flood risk.

Figure 7: Breakdown of flood average annual loss and loss ratio % by region



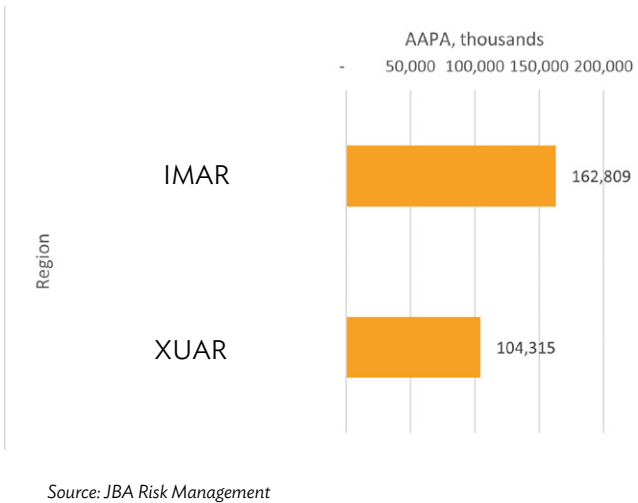
Source: JBA Risk Management

Figure 8: Average annual fatalities - flood



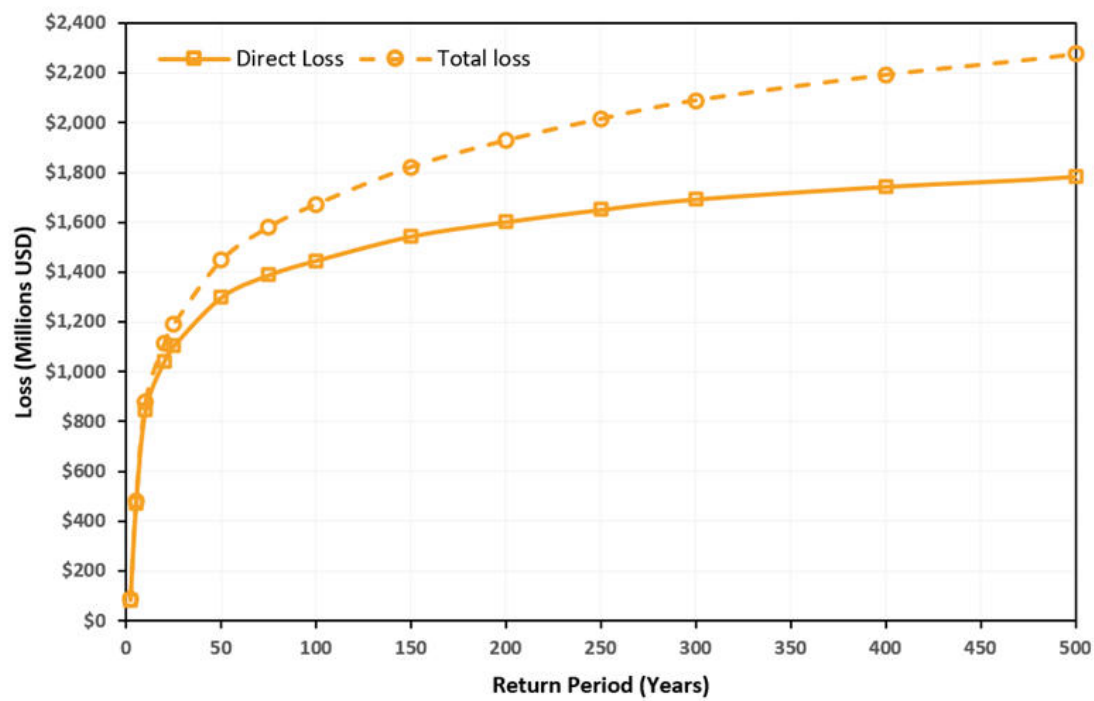
Average annual fatalities from floods is 8 in IMAR and 5 in XUAR. Despite IMAR's population of 24.2 million, average annual fatalities are low since many population centres are in areas of low flood risk. Fatalities in XUAR are also low due to the predominantly arid climate and the small number of major rivers in the region. Figure 8 provides details on average annual fatalities in the two regions.

Figure 9: Average annual number of people affected - flood



As seen in Figure 9, the average annual number of people affected by floods in IMAR is 162,809 which is less than 0.01% of the total population of the region. In XUAR, the average annual number of people is 104,315 which is less than 0.005% of the region's total population.

Figure 10: Exceedance probability curves – floods – IMAR

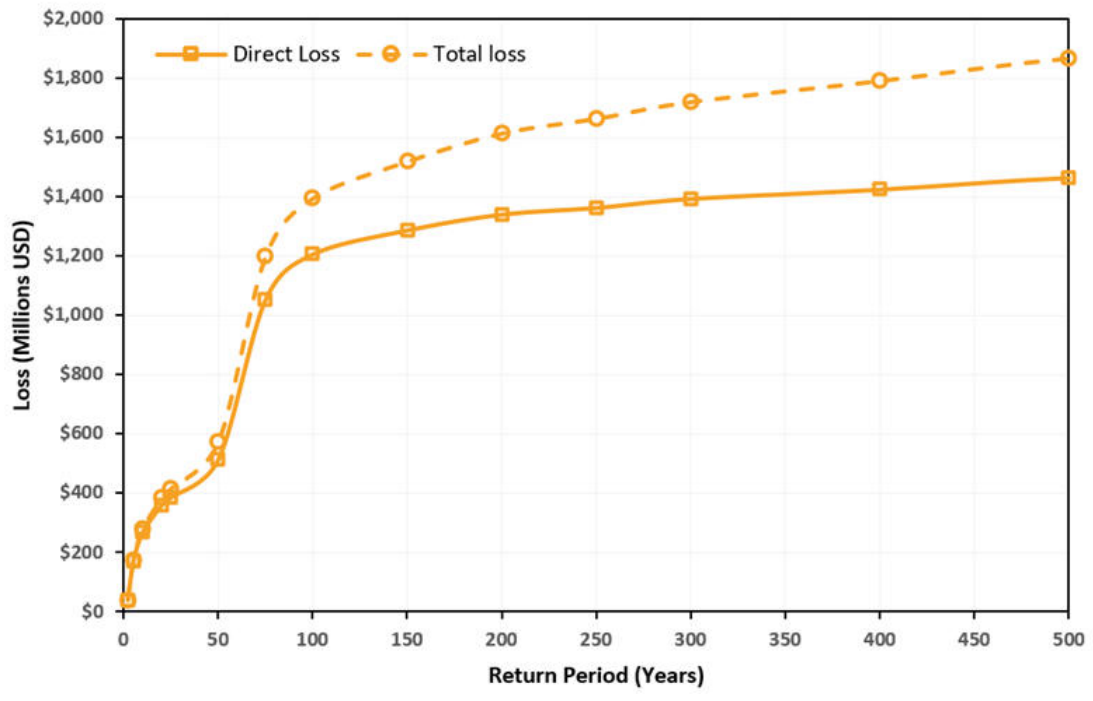


Source: JBA Risk Management.

The flood exceedance probability (EP) curves show the total and direct loss from all events for the given return periods. In Figure 10, the EP curves for IMAR show that loss increases most significantly between the 2 and 50-year return periods. At the 100-year return period, direct loss from floods is modeled at just under \$1.5 billion, which is around 0.5% of the

region’s GDP. Above the 100-year return period, direct loss increases at a lower rate, reaching up to \$1.79 billion at the 500-year return period. The EP curve for total loss shows that is modeled to continue to rise to nearly \$2.3 billion at the 500-year return period.

Figure 11: Exceedance probability curves – floods – XUAR



Source: JBA Risk Management.

The EP curves for floods in XUAR in Figure 11 show that loss increases most notably between the 50 and 75-year return periods, from just over \$500 million to over \$1 billion, respectively, which suggests a sensitivity to flood events in this range of return periods. At the 100-year return period direct loss is modeled at \$1.2 billion, which is around 0.6%

of XUAR’s nominal GDP. Direct loss increases at a much lower rate above the 100-year return period, reaching close to \$1.5 billion at the 500-year return period. Total loss continues to increase at a steady rate beyond the 100-year return period, reaching nearly \$1.9 billion for the 500-year event.

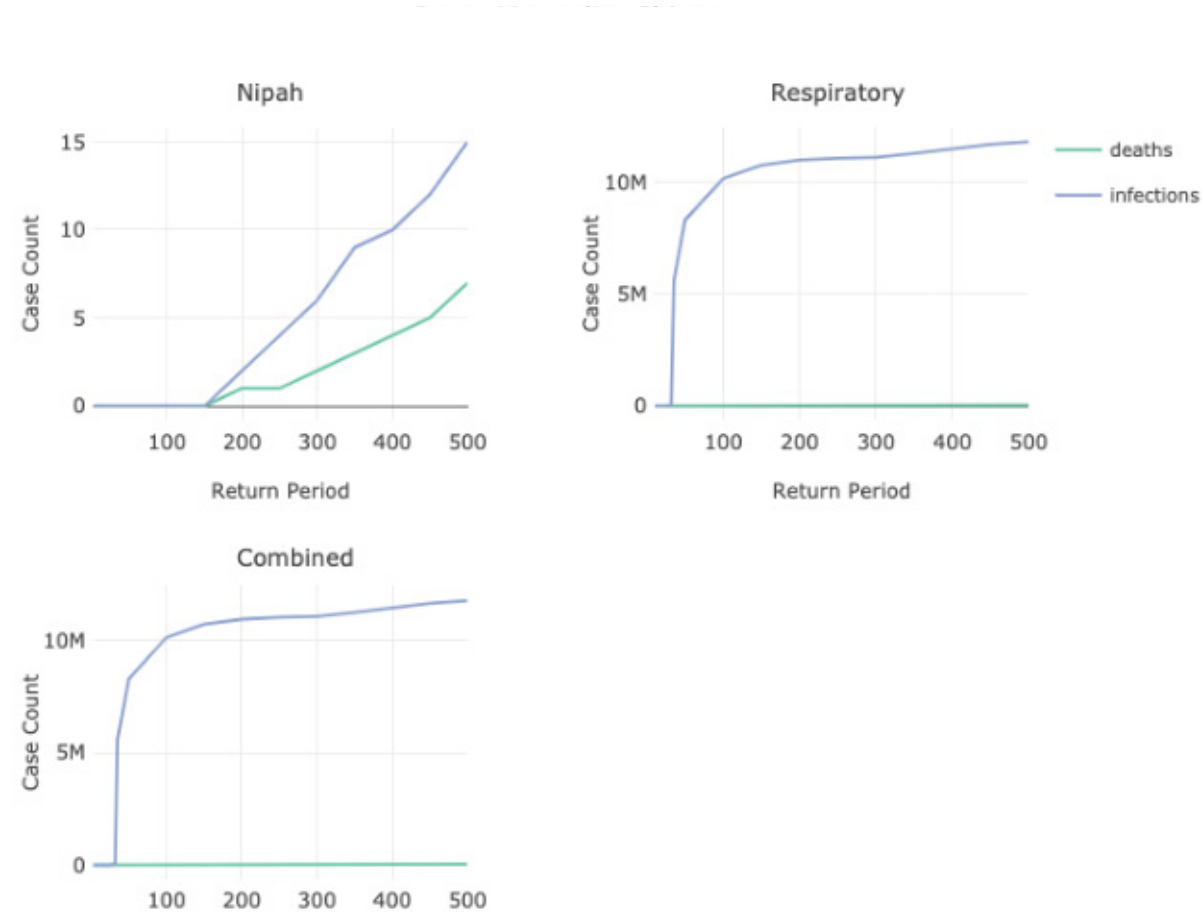


Infectious disease

The modeled EP curves include only those infections and deaths that are in excess of the regularly occurring annual baseline. For the included respiratory diseases like pandemic influenza and novel coronaviruses, this baseline will be zero, but

for diseases like Crimean-Congo Haemorrhagic Fever (CCHF), which is endemic in some CAREC countries, the baseline will be higher than zero. Box 2 highlights the pathogens modeled as part of this analysis.

Figure 12: Exceedance probability curves – pandemic, including CCHF, Nipah virus infection, respiratory viruses and combined (all pathogens) – IMAR

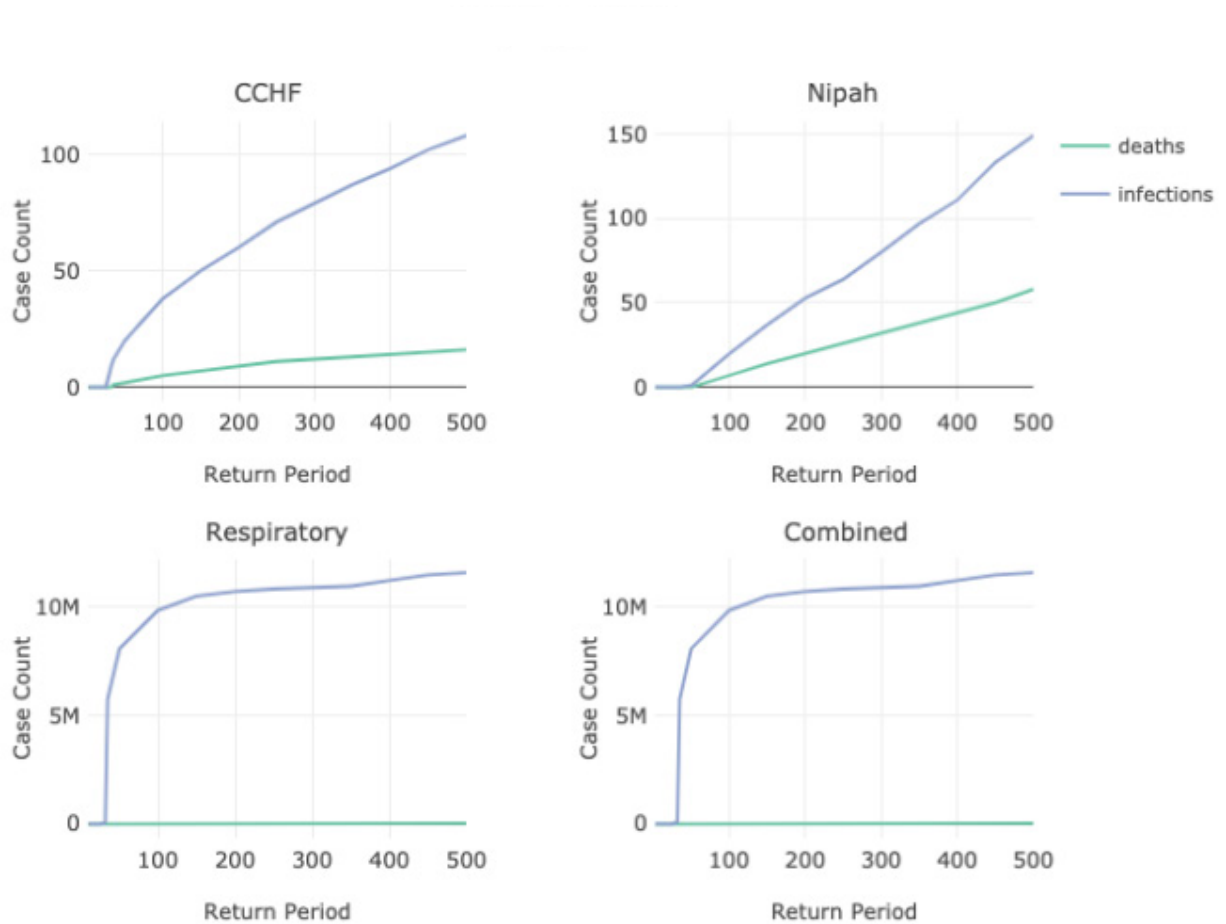


Source: Metabiota. Note that the graph for CCHF in IMAR was omitted due to low risk in this region.

The pathogen EP curves in Figure 12 and 13 for IMAR and XUAR highlight that respiratory pathogens account for most of the epidemic risk in both areas. The curve climbs rapidly and steeply because respiratory pathogens tend to be highly transmissible and cause very large pandemics when they occur (COVID-19 and pandemic influenza are notable examples).

CCHF and Nipah virus have much lower transmission leading to much smaller outbreaks which is consistent with what is shown in the EP curves: a few cases showing up at higher return periods for both regions. Table 1 details the average annual infections and deaths from these pathogens.

Figure 13: Exceedance probability curves – pandemic, including CCHF, Nipah virus infection, respiratory viruses and combined (all pathogens) – XUAR



Source: Metabiota.



Table 1: Average annual losses - pandemic, including CCHF, Nipah virus infection, respiratory viruses and combined (all pathogens)

Pathogen	IMAR		XUAR	
	AAL - Infections	AAL - Deaths	AAL - Infections	AAL - Deaths
Combined	275,707	405	268,488	406
Respiratory	275,705	404	268,443	390
Nipah	2	1	44	16
CCHF	<1	<1	1	<1

Source: Metabiota

**Box 2: Pathogens modeled**

- Respiratory: a range of novel respiratory pathogens are included such as pandemic influenza, emergent coronaviruses (Severe Acute Respiratory Syndrome (SARS) and Middle East Respiratory Syndrome (MERS)). This does not include endemic pathogens such as measles. A re-emergence of SARS-CoV-1 or a new SARS coronavirus are included.
- Crimean-Congo haemorrhagic fever is caused by a tick virus is transmitted by tick bites or through contact with infected animal blood or tissues. Symptoms include fever, muscle ache and pain, dizziness, nausea, vomiting, diarrhea,

sleepiness, and depression. The case fatality rate is estimated between 10-40%. Some medicines seem to be effective<sup>2</sup>

- Nipah virus is a zoonotic virus (it is transmitted from animals to humans) ; it is also transmitted through food or people. It can cause a range of illnesses, from asymptomatic infection to severe respiratory illness and fatal encephalitis. The case fatality rate is estimated between 40-75% and there is currently no treatment or vaccine available.<sup>3</sup>

<sup>2</sup> <https://www.who.int/news-room/fact-sheets/detail/crimean-congo-haemorrhagic-fever>  
<sup>3</sup> <https://www.who.int/news-room/fact-sheets/detail/nipah-virus>



# Historical losses and impacts

**Inner Mongolia Autonomous Region and Xinjiang Uygur Autonomous Region are two of the largest administrative subdivisions within the PRC, each with distinctive topography and natural hazards. The plateau of IMAR and the deserts and grasslands of XUAR also create a specific urbanization pattern. The Himalayas spans the southern border with India and Nepal, the Tianshan range crosses central XUAR, and the Yinshan range extends across the middle section of the IMAR Plateau.**

In the past three decades, floods and earthquakes combined are estimated to have affected over 3.5 million people and resulted in over \$1.1 billion in damage (Table 2).

**Table 2: Total impacts from floods and earthquakes, 1990-2019**

	Fatalities	Number of people affected	Total damage (\$ million; constant 2019)
<b>IMAR</b>			
<b>Flood</b>	265	210,000	6315.51
<b>Earthquake</b>	22	857,900	241
<b>XUAR</b>			
<b>Flood</b>	615		4635.31
<b>Earthquake</b>	390	2,602,016	825

Source: EM-DAT

XUAR is predominantly arid. Two vast inland river basins, namely the Tarim Basin and Junggar Basin, cover an area of 1,020,000 km<sup>2</sup> and 777,000 km<sup>2</sup>, respectively. Heavy rainfall, sometimes combined with snowmelt, can trigger flooding, which leads to significant damage and loss of lives. In 2002, XUAR suffered a flood event causing 11 deaths.

Rainfall-induced floods are a frequent hazard in IMAR during the East Asian Monsoon season. In July 2018, IMAR experienced some of the most significant flooding in recent years, with an estimated 761,000 people affected, 12 people killed, and CNY 5.3 billion (\$ 778 million) in economic losses incurred.<sup>4</sup> In June 2012, flooding caused \$102 million of direct economic loss and 19 fatalities.<sup>5</sup>

A flood in October 1998 affected 6.19 million people which left 375,400 homeless. This flood event, one of the greatest in IMAR, resulted in losses totalling to \$2.15 billion (CNY 15.1 billion in 1998).<sup>6</sup>

In July 2018, torrential rainfall led to 20 fatalities in the northwest of the region around Qincheng Township in Hami, with damage to infrastructure, farmland, and 8,700 houses. Rainfall of 110mm fell in one hour leading to the breach of a dam designed to withstand rainfall with a return period of 300 years.<sup>7</sup>

<sup>4</sup> Akipress (2018) China allocates flood relief funds for Sichuan, IMAR [https://akipress.com/news/609659:China\\_allocates\\_flood\\_relief\\_funds\\_for\\_Sichuan,\\_Inner\\_Mongolia/](https://akipress.com/news/609659:China_allocates_flood_relief_funds_for_Sichuan,_Inner_Mongolia/)

<sup>5</sup> ReliefWeb (2012) Rain-triggered floods leave 19 dead in Inner Mongolia <https://reliefweb.int/report/china/rain-triggered-floods-leave-19-dead-inner-mongolia>

<sup>6</sup> Ge et al., 2017 [online]. Available from: <https://onlinelibrary.wiley.com/doi/pdf/10.1111/jfr3.12160>

<sup>7</sup> ReliefWeb (2018) 20 dead, 8 missing as record heavy rain triggers floods in Xinjiang <https://reliefweb.int/report/china/20-dead-8-missing-record-heavy-rain-triggers-floods-xinjiang>

**Table 3: The most impactful flood and earthquake events, 1900 – 2019**

Year	Location	Economic losses (\$ millions)	Fatalities	Number of people affected
<b>Floods</b>				
<b>2002</b>	XUAR		500	
<b>2016</b>	IMAR	4309.99	164	
<b>2012</b>	IMAR	1357.55	91	
<b>2003</b>	XUAR		51	
<b>2014</b>	IMAR	647.97	10	
<b>Earthquakes</b>				
<b>1931</b>	XUAR		10,000	
<b>1902</b>	XUAR		2,500	
<b>1906</b>	XUAR		280	
<b>2003</b>	XUAR		261	
<b>1924</b>	XUAR		100	
<b>2004</b>	IMAR	74		

Source: EM-DAT with validation from other sources including Swiss Re, ReliefWeb, World Bank reports for floods; NOAA Significant Earthquakes database for earthquakes

**Table 4: Notable infectious disease outbreaks, 1990-2021**

Prior to the COVID-19 outbreak, both IMAR and XUAR had infectious disease outbreaks with XUAR experiencing several small CCHF events.

Pathogen	Date first case reported	Date last case reported	Total cases	Total deaths	Location of origin
<b>IMAR</b>					
<b>SARS Coronavirus</b>	19 Mar 2003	31 May 2003	309	0	PRC
<b>2019 Novel Coronavirus (2019-nCoV)</b>	24 Jan 2020	21 Oct 2020	275	0	PRC
<b>XUAR</b>					
<b>CCHF virus</b>	1 Jan 2001	30 June 2001	51	3	PRC
<b>CCHF virus</b>	1 Jan 1965	31 Dec 1965	11	10	PRC
<b>CCHF virus</b>	1 Jan 1966	30 June 1966	8	6	PRC
<b>2019 Novel Coronavirus (2019-nCoV)</b>	24 Jan 2020	21 Oct 2020	901	0	PRC

Source: Metabiota's infectious disease database



# Hazard

**The distinct landscape across IMAR and XUAR brings a varying hazard profile. Mountain ranges, deserts, dry grasslands and a plateau all affect the seismic and flood hazard geographic pattern.**

## Seismic hazard

In the IMAR region, the largest instrumentally observed earthquake occurred on a strike-slip fault structure in the proximity of the southern border, close to the city of Zhangye.

During the last century, the largest magnitude earthquakes were concentrated in the central and southern parts of the country, particularly in the area of Baotou and Datong. The ISC-GEM catalogue contains 5 earthquakes that occurred between 1929 and 1954 with magnitudes in the range between 6 and 6.86.<sup>8</sup>

XUAR has experienced intense seismic activity since 1900. According to the ISC-GEM catalogue<sup>9</sup> more than 70 earthquakes of magnitude 6.0 and larger occurred in this region since the early 1900s. Most of the seismicity occurred within the mountain ranges that cross the autonomous regions from east to west. The central area of the region, approximately corresponding to the cratonic Tarim Basin, shows notably lower rates of seismicity than the rest of its territory. The largest instrumentally recorded earthquake in XUAR is the 1906 Manas earthquake (magnitude 7.95), which occurred in the Northern Tian Shan belt along a thrust fault.

The highest hazard for IMAR in terms of the peak ground acceleration with a 10% probability of exceedance in 50 years (PGA10%50yr) on reference site conditions ( $V_{s30}$  of 800 m/s) is in a small area close to Bayannur, seemingly controlled by one of the faults of the Yinchuan Graben. The rest of the region shows values of PGA10%50yr lower than 0.1g; in Baotou, this parameter has values in the order of 0.1g.

In XUAR, the largest values of the peak ground acceleration with a 10% probability of exceedance in 50 years (PGA10%50yr) on reference site conditions ( $V_{s30}$  of 800 m/s) are in the Kunlun Shan southern part of the country. The areas of lower hazard are the three main plains, namely the Tarim pendi, the Turpan pendi and, to a minor extent, the Junggar pendi. In these sectors, the PGA10%50yr does not exceed 0.1g while in Urumqi it is slightly above 0.2g.

## Hydrological catchment areas

Exposure to flooding can be assessed via hydrological accumulation zones (HAZ). HAZ polygons represent the natural watercourse boundaries as a means of modeling the flow of water. The HAZ polygons for IMAR give the structure of the hydrological basins across the country. Much of IMAR is dry with few significant watercourses, away from the northeast of the region. Flows tend to be ephemeral and flash flooding from heavy rainfall tends to be the main hazard.

The HAZ polygons for the XUAR region show a large area of very narrow HAZ polygons in the southwest which represent narrow valleys with little or no flow. These show that there are arid desert or mountains with very low flows in rivers which often run dry.



<sup>8</sup> (version 7.0 - see <http://www.isc.ac.uk/iscgem/>)

<sup>9</sup> (version 7.0 - see <http://www.isc.ac.uk/iscgem/>)



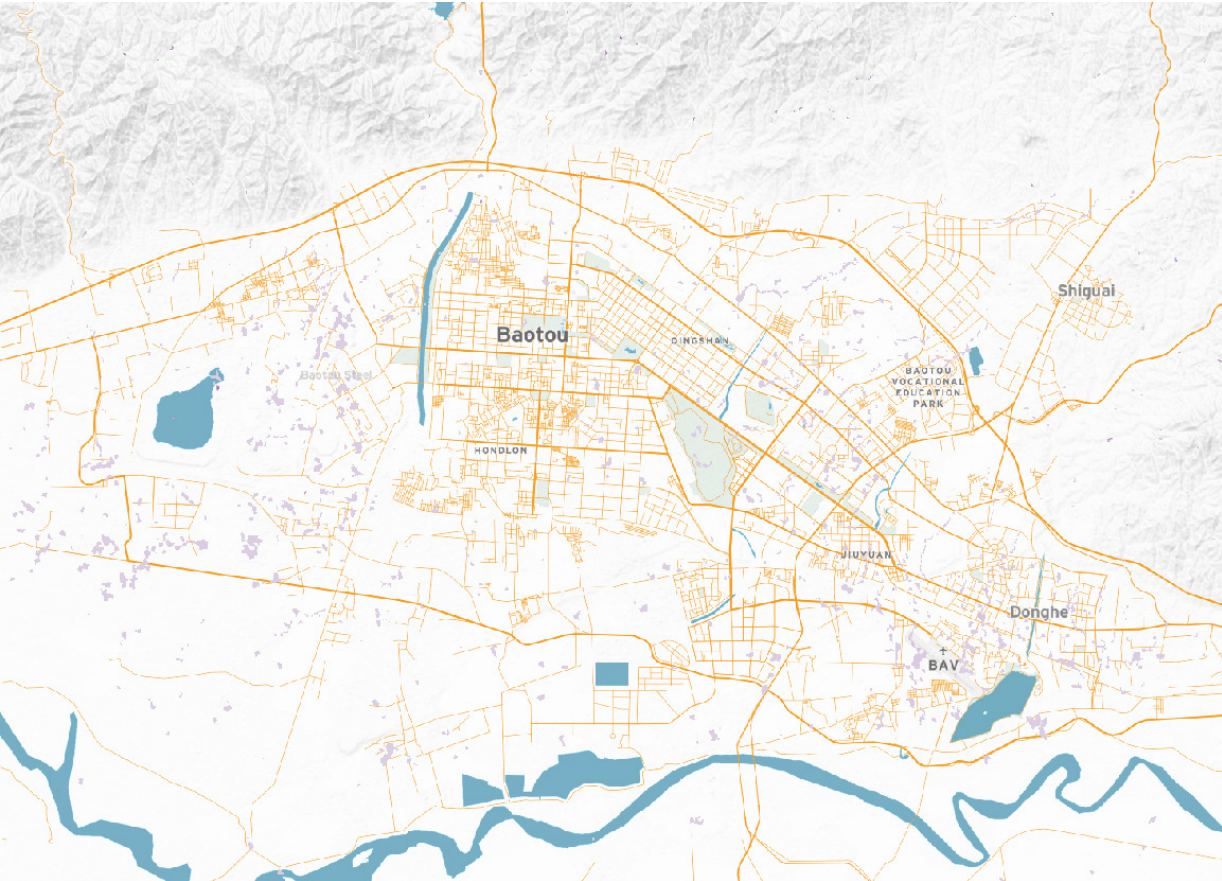
Flood hazard map for pluvial and fluvial flooding

Flood modelling estimates losses and impacts on the basis of flood maps for river (fluvial) and surface water (pluvial) flooding generated at 30 metre spatial resolution. These maps use observed river and rainfall data to generate extreme rainfall and river flow volumes. Maps are generated for different return periods. The 1 in 200-year return period river flood map highlights the main rivers across IMAR and XUAR. This event severity is often used for planning purposes as a plausible extreme event

In the west of IMAR, river valleys are dry outside of periods of rainfall and flood risk to people is very limited due to the sparse population. The Yellow River crosses the region’s southern border just south of Wuhai and runs south and then east past Baotou in a broad valley before heading south across the IMAR boundary. It is joined near Hohhot by the Dahei River which runs along the southern edge of the city. Central and northern parts of the region also have some significant river valleys and flood plains; however, like in the west of IMAR very few population centres are threatened by river flooding.

In XUAR, any rainfall in the west of the region drains from high ground into the Aksu and Hotan Rivers which flow west to the Tarim River; the rainfall’s impacts on the population is limited. The north of XUAR is similarly arid with few major rivers. The drainage pattern of XUAR is unique within the PRC. The only stream whose waters reach the sea is the Irtys River, which rises in north-central XUAR (as the Ertix River), flows west and crosses into Kazakhstan, and, as the Irtys, flows through the Russian Federation into the Ob River, which then empties into the Arctic Ocean.

Figure 14: Map of surface water (pluvial) flooding (areas in purple) at the 200-year return period level for the Baotou region

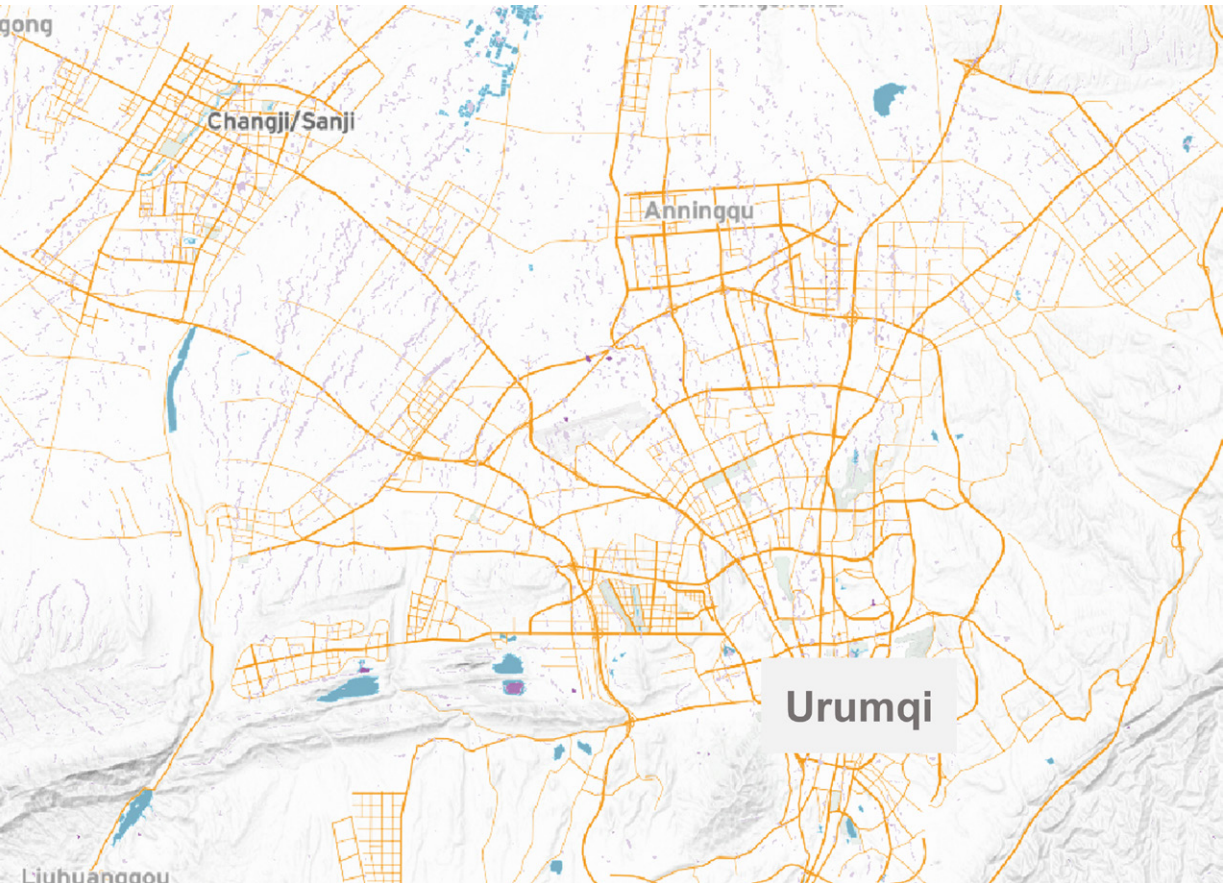


Source: JBA

The flood map of Baotou in Figure 14, the largest city in IMAR, shows areas of surface water flooding to the west of the city in mainly industrial areas and to the southeast of the city in the mixed residential and commercial districts close to the airport.



**Figure 15: Map of surface water (pluvial) flooding (areas in purple) at the 200-year return period level for the Urumqi region**



Source: JBA

In Figure 15 the surface water flood map for Urumqi shows very small low exposure. Risk is concentrated in small areas away from the built-up regions.

Climate conditions

Historic climate

Vast grasslands span the majority of IMAR, with precipitation levels decreasing from east (> 500mm per year) to west (< 250mm annually).<sup>10</sup> Vegetation types shift along this semi-humid gradient from meadow steppe to desert steppe in the arid areas to full desert in the northwest corner. The East Asian Monsoon brings warm and moist air from the south to bring summer rains to the northeast of the autonomous regions. The Siberian anticyclone leads to cold and relatively dry winters.

Seasonal temperature variation is large, ranging from over 40°C in summer to -20°C in winter. Minimum and maximum mean temperatures and the number of extreme heat events have been increasing.<sup>12</sup> Annual mean temperatures have increased by approximately 0.4°C per decade over the period 1960-2010.

Decreases in mean precipitation totals during the primary grass growing season (around April to September and associated with the East Asian Monsoon) have been observed since the 1960s.<sup>13</sup> It is not yet possible to detect a clear climate change signal in the decreasing East Asian precipitation trends for IMAR as the monsoon system is modulated by inter-decadal climate patterns such as the Pacific Decadal Oscillation. At the same time, however, an increasing proportion of the spring and summer rains has been falling as extreme heavy rainfall events which contribute to flooding and

grassland damage. On the other hand, the incidence and intensity of drought has increased since the 1990s, particularly during the summer and autumn seasons. When these droughts extend through the winter — known as ‘black disaster’ droughts — they are particularly brutal for livestock survival and herder livelihoods.

XUAR’s climate zones range from high mountain alpine to semi-arid to desert, with annual mean precipitation greatest over the Tianshan and Altay mountain regions<sup>14</sup>. Summer precipitation around June to September contributes to the largest proportion of annual precipitation totals for many parts of the autonomous regions. It is linked with water vapour advected from the eastern PRC and from the Indian Ocean (via westerlies) rather than the East Asian Monsoon.<sup>15</sup> Urban areas and communities are clustered around the Tarim and Junggar rivers, whose flows are sustained by winter snowpack and glacier melt from the mountains.

<sup>10</sup> Pan, X., Q. Li, et al. (2016) Grasslands and Livestock. In: *Climate Risk and Resilience in China*. R. Nadin, S. Opitz-Stapleton and Y. Xu [Eds.], Routledge: London.  
<sup>11</sup> Yatagai, A., K. Kamiguchi, et al. (2012) ‘APHRODITE: Constructing a long-term daily gridded precipitation dataset for Asia based on a dense network of rain gauges’. *BAMS*, doi:10.1175/BAMS-D-11-00122.1  
<sup>12</sup> Hang, S., P. Shan, et al. (2016) Climate change and Inner Mongolia. In: *Climate Risk and Resilience in China*. R. Nadin, S. Opitz-Stapleton Y. Xu [Eds.], Routledge: London.  
<sup>13</sup> Wang, G., R. Nadin and S. Opitz-Stapleton (2016) A balancing act: China’s water resources and climate change. In: *Climate Risks and Resilience in China*. R. Nadin, S. Opitz-Stapleton and Y. Xu [Eds.], Routledge: London.  
<sup>14</sup> Zhu, X., M. Zhang, et al. (2015) ‘Comparison of monthly precipitation derived from high-resolution gridded datasets in arid Xinjiang, Central Asia’. *Quaternary International*: <https://doi.org/10.1016/j.quaint.2014.12.027>  
<sup>15</sup> Zhou, Y., Z. Xi and X. Liu (2019) ‘An analysis of moisture sources of torrential rainfall events over Xinjiang, China’. *Journal of Hydrometeorology*: doi:10.1175/JHM-D-19-0010.1



Weather station data is limited and observing trends in precipitation and temperature challenging. Trends in annual precipitation between 1950 and 2010 over XUAR are spatially inconsistent but have generally been observed to be increasing over the mountain areas since the 1960s,<sup>17</sup> largely related to summer precipitation increases of 1 to >3mm/year since the late 1970s. Summer flood frequency has also been observed to be increasing since the early 1980s<sup>18</sup> and is linked to shifts in extreme precipitation events.

**Future precipitation projections**

Two Regional Climate Model-Global Climate Model (RCM-GCM) simulations from the Coordinated Regional Climate Downscaling Experiment (CORDEX) East Asia domain were used to examine climate change impacts on precipitation. Two Representative Concentration Pathways (RCP4.5 and RCP8.5) were selected; these respectively represent a medium and high (business as usual) emissions pathway, respectively. The RCMs were bias corrected before precipitation projection analysis of how conditions could shift between the 2050s (2031-2070) and a historical reference period of 1956-1995. The multi-model mean information was used to examine yearly and seasonal changes under RCP4.5 and RCP8.5.

Precipitation extremes from each model and RCP were individually used to calculate future precipitation intensities, which is relevant to estimating future flood risk. Box 3 describes the methodology behind the future climate calculations. The area-averaged annual maximum rainfalls for 24-hr duration for each province was extracted and analyzed for different return periods (2, 5, 10, 20, 50, 100, 500-, 1000-, 5000- and 10000-year events).

Mean annual temperatures are also increasing over the period of 1979-2011 throughout XUAR, although spatial rates of change vary. In the mountain zones, temperatures have increased an average of 0.3 to 0.6°C/decade.<sup>19</sup> They have been increasing in the Tarim basin since 1980s roughly from 0.6 to 0.9°C/decade. This change is related to increases in spring minimum and maximum temperatures,<sup>20</sup> which lead to increasing frequency of temperature-related snowmelt-induced flooding.

Multiple climate change studies indicate that the East Asian monsoon might become more variable; trends in future winter precipitation are unclear and dependent on the model and the emission pathway. The multi-model projection means for both RCP4.5 and RCP8.5 indicate that summer (July to September) mean precipitation could decrease by 10 to 20% for parts of eastern IMAR, though the spatial patterns of decrease are different. Under both emissions pathways, summer mean precipitation in the 2050s could increase by 10 to 70% for parts of Alxa League, Wuhai and Bayannur.

Overall annual precipitation might not change much for most of the autonomous regions by the 2050s in comparison with annual means between 1956-1995. Potential increases are noted in the west due to potentially more precipitation during both the summer and the winter (January to March). Winter precipitation is also projected to increase by up to 20% under both RCPs for Hulunbuir.

Multi-model mean projections of 24-hr duration precipitation intensity shifts are spatially different between RCP4.5 and RCP8.5. Under RCP4.5 the intensities of 24-hr extremes could slightly decrease for Alxa, Bayannur, Higgan League, Hohhot, Hulunbuir, and Xilingol League. Extreme intensities under RCP8.5 could potentially decrease for Higgan League, Hulunbuir, Ulanqab and eastern Xilingol League.

<sup>16</sup> Yatagai, A., K. Kamiguchi, et al. (2012) 'APHRODITE: Constructing a long-term daily gridded precipitation dataset for Asia based on a dense network of rain gauges'. BAMS: doi:10.1175/BAMS-D-11-0012.1  
<sup>17</sup> L. Xu, H. Zhou, et al. (2015) 'Precipitation trends and variability from 1950 to 2000 in arid lands of Central Asia'. Journal of Arid Land: <https://doi.org/10.1007/s40333-015-0045-9>  
<sup>18</sup> Zhang Q., X. Gu, et al. (2015) 'Magnitude, frequency and timing of floods in the Tarim River Basin, China: Changes, causes and implications'. Global and Planetary Change: doi:10.1016/j.gloplacha.2015.10.005  
<sup>19</sup> Hu Z., C. Zhang, et al. (2014) 'Temperature changes in Central Asia from 1979 to 2011 based on multiple datasets'. Journal of Climate: doi:10.1175/JCLI-D-13-00064.1  
<sup>20</sup> Feng R., R. Yu, et al. (2017) 'Spatial and temporal variations in extreme temperature in Central Asia'. International Journal of Climatology: doi:10.1002/joc.5379





Table 5 below shows projected changes in 24-hr duration extreme precipitation intensities in Baotou for 2031-2070 (the 2050s) as compared to historical 24-hr intensities of different return periods. The table shows the median of the multi-model ensemble and the 25th and 75th percentiles in brackets. Box 3 describes the methodology behind the future climate calculations.

Multi-model climate change projections indicate that XUAR's annual mean precipitation could increase by 10 to 40% over the Kunlun Mountains and the southern borders of the Taklamakan Desert under both RCP4.5 and RCP8.5 by the 2050s when

compared with annual means from 1956-1995. Potential drying between -10 and -20% is seen for sections of the Taklamakan and the drier areas of the Tarim River Basin in the north. Shifts in the annual means are reflected in seasonal totals. Drying ranging from -10 to -20% is projected during the summer (July to September) and greater under RCP8.5 than RCP4.5 while precipitation increases of up to 40% are seen over the southern third of the region. These projections are consistent with other climate change studies for XUAR, which have largely projected drier conditions over the desert areas and precipitation increases over some of the higher elevation areas.

Table 5: Baotou 24-hr duration extreme precipitation intensity (mm/hr)

Return period	1951-2007	2050s	
	Historical	RCP4.5	RCP8.5
20-year	1.08	1.30 (1.23, 1.35)	1.38 (1.30, 1.44)
100-year	1.51	1.64 (1.54, 1.71)	1.92 (1.78, 2.02)
200-year	1.69	1.78 (1.68, 1.86)	1.92 (1.78, 2.02)
500-year	1.92	1.97 (1.85, 2.06)	2.13 (1.97, 2.26)

While mean summer precipitation is projected to decrease over much of XUAR, the intensity of short-duration extreme precipitation events is likely to increase under both RCP4.5 and RCP8.5 according to multi-model projections, though RCP8.5 shows smaller intensity increases. Extremes' intensities are projected to increase more over the mountainous areas of XUAR than over

the desert areas. For instance, in Shihezi City what was once the ~400-year rainfall event could shift to the 100-year event and the ~100-year event could become the 1 in 20-year event. Similar shifts are seen in extreme precipitation events for Urumqi as shown in Table 6. It is these short-duration extreme rainfall events that bear great responsibility for flash flooding, infrastructure and agricultural damage, and loss of life.

Table 6: Urumqi 24-hr duration extreme precipitation intensity (mm/hr)

Return period	1951-2007	2050s	
	Historical	RCP4.5	RCP8.5
20-year	0.73	0.88 (0.85, 0.83)	0.80 (0.77, 0.83)
100-year	0.99	1.16 (1.10, 1.23)	1.04 (0.98, 1.08)
200-year	1.10	1.27 (1.21, 1.36)	1.14 (1.06, 1.19)
500-year	1.25	1.44 (1.35, 1.54)	1.27 (1.19, 1.33)

Table 6 shows projected changes in 24-hr duration extreme precipitation intensities in Urumqi for 2031-2070 (the 2050s) as compared to historical 24-hr intensities of different return periods. The

table shows the median of the multi-model ensemble and the 25th and 75th percentiles in brackets. Box 3 describes the methodology behind the future climate calculations.

Box 3: Future climate methodology

- Climate change impacts on precipitation were examined by use of Regional Climate Models. Two Representative Concentration Pathways (RCPs) were selected: RCP 4.5 as a medium emissions pathway and RCP 8.5 as a high (business-as-usual) pathway.
- Multi-model projections simulated how precipitation could differ in the 2050s compared to the historical reference period of 1956-1995. Precipitation projections were made to examine how conditions could differ

in the 2050s to the historical reference period of 1956-1995. This reference period accounts for two phases of the Atlantic Multidecadal Oscillation, which modulates climate over Central Asia. The 2050s were chosen as a policy relevant period where a climate change signal is detectable.

Further information on the approach is detailed in the Technical Documentation

# Exposure

**The make-up, structure and location of economic development dictates the value at risk and the nature of exposure to natural hazard events.**

IMAR is one of the most economically developed autonomous regions in the PRC with annual GDP per capita close to \$ 13,000. XUAR has traditionally been an agricultural region with lower GDP per capita.

Table 7: Population totals, distribution and trends

Population (thousands)	1,397,715.00 (2019)*
IMAR Population (thousands)	24,706,321 (2010)**
XUAR Population (thousands)	21,813,334 (2010)**
Population growth rate (%/year)	0.4 (2019)*
Share of population living in urban areas (%)	60 (2019)*
Urbanisation rate (%/year)	2.3 (2019)*
% of total population age 0-14	18 (2019)*
% of total population age 15-64	71 (2019)*
% of total population ages 65 and above	11 (2019)*

Note: \*Figures are for PRC total. Source: World Bank Open Data except \*\*source: Britannica.com

IMAR stretches across the northern part of the PRC and covers almost one-third of the country's grasslands and about one-fourth of its pasture area. In 2015, the forest area in IMAR reached 24.9 million hectares, accounting for 21 percent of the total surface area. Much of the western territory is barren, characterized by shifting sands and sparse vegetation.

IMAR, traditionally agricultural and pastoral, has become much more urbanized since the late 1990s, especially around the three major urban areas located in the centre of the region. Baotou is a large industrial complex and transportation hub west of Hohhot; Hohhot is the region's political and cultural centre; and Jining is a commercial and transportation centre east of the capital. About half of IMAR's population is now classified as urban, with main population densities sitting on the southern border of the region.

The Tian Shan mountain ranges occupy nearly one-fourth of the area of XUAR. The mountains, which are dominated by pine forests, stretch into the region from Kazakhstan, Kyrgyz Republic, and Tajikistan and run eastward from the border for over 1,500km. Because of the dry climate, most of the cultivated land in XUAR depends entirely on irrigation. Vast areas of the south of the region compromise the Takla Makan, a near barren desert covering an area of approximately 123,550 square miles (320,000 square km).

XUAR has a number of significant population centres. Urumqi, the regional capital and Karamay, are both in central Xinjiang along the northern foothills of the Tian Shan, whilst Shihezi sits south of those areas.

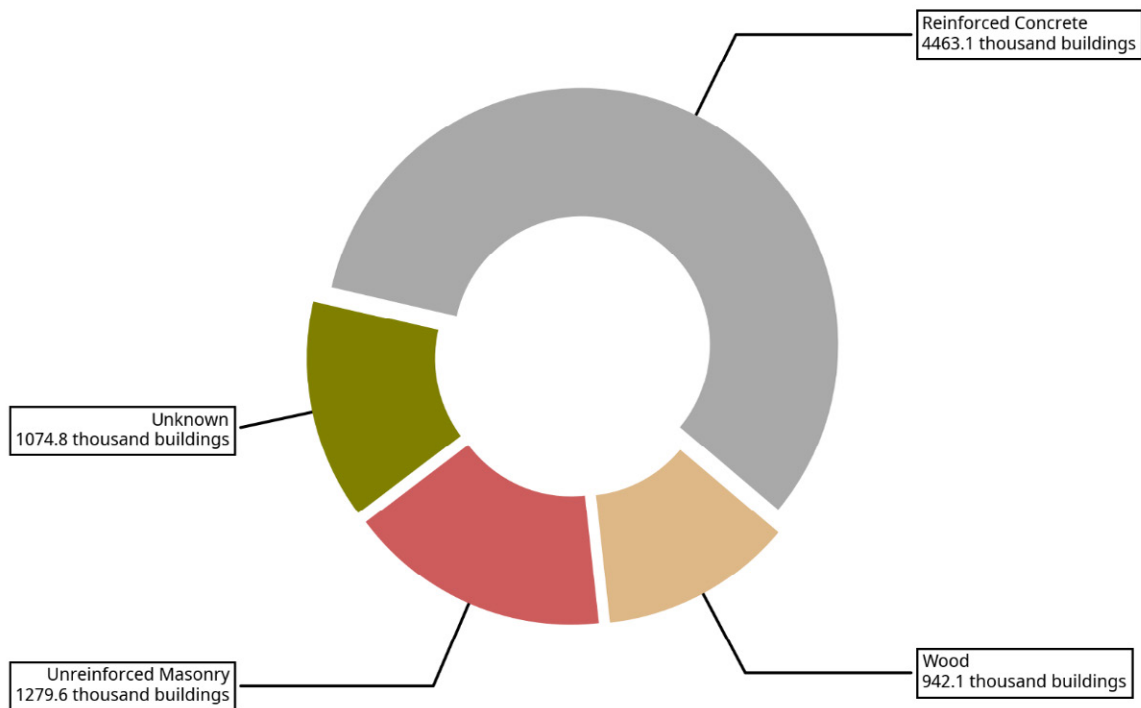
Table 8: Key economic indicators

GDP (million USD, current)	14,342,902.84 (2019)*
IMAR GDP (million USD, current)	279,000,000,000 (2020)
XUAR GDP (million USD, current)	211,000,000,000 (2020)
GDP per capita (USD, current)	10,261.70 (2019)*
IMAR GDP per capita (USD, current)	13,000 (2019)
XUAR GDP per capita (USD, current)	2,898 (2009)
Country / territory economic composition	
Agriculture, forestry and fishing, value added (% of GDP)	7.1 (2019)
Employment in agriculture (% of total employment) (modeled ILO estimate)	25 (2020)
Industry (including construction, value added (% of GDP)	39 (2019)
Employment in industry (% of total employment) (modeled ILO estimate)	28 (2020)
Services, value added (% of GDP)	53.9 (2019)
Employment in services (% of total employment) (modeled ILO estimate)	47 (2020)

Note: \*Figures are for total PRC. Source: World Bank Open Data



Figure 16: Breakdown of building types – PRC



As seen in Figure 16, the PRC is estimated to have a total of 7,436,381 residential buildings valued at \$476.0 billion, 1,055,514 commercial buildings valued at \$60.3 billion, and 559,650 industrial buildings valued at \$30.2 billion.

Reinforced concrete structures with an estimated total of 4,463,074 buildings make up the largest fraction (57.5%) of the total building stock across the PRC. This is followed by unreinforced masonry structures (1,279,601 buildings, or 16.5%) and non-engineered structures of various types including adobe, stone masonry and unknown construction materials (1,074,827 buildings, or 13.9%).

In IMAR, exposure is centred around Baotou, which developed into one of the major iron-and-steel producers in the PRC. Other major industrial centres include the capital and most populous city Hohhot, Chifeng, and, to the west, Wuhai. XUAR has traditionally been an agricultural region with much lower exposed assets.





# Vulnerability

**T**he social impacts of hazard events are greatly affected by the structure and organization of societies and economies. Vulnerability can be thought of as one determinant of disaster risk, the other being the natural hazard event. The structure of politics, economics and livelihoods affects vulnerability to disaster events. Policy

and investment choices can increase or decrease vulnerability, and so determine the overall level of disaster risk. Deliberate policies, such as for disaster risk reduction and finance, can reduce vulnerability. Other forces, such as pattern of urbanisation or decline of ecosystem services, may unintentionally increase vulnerability.

**Table 9: Socio-economic vulnerability indicators**

Poverty headcount ratio at national poverty lines (% of population)	0.6 (2019)
Human Capital Index	0.7 (2020)
GINI index	38.5 (2016)
Gender Inequality index	0.16 (2018)
Household size	3.4 (2019)
Age dependency ratio (% of working age population)	41 (2019)
Unemployment rate (modeled ILO estimate)	4.4 (2020)
General government gross debt (% of GDP)	48.796 (2018)
Under five child mortality (per 1000 live births)	8 (2019)
Life expectancy at birth (female)	79 (2018)
Life expectancy at birth (male)	75 (2018)
% of population using at least basic sanitation services	85 (2017)
% of population using at least basic drinking water services	93 (2017)

Source: World Bank Open Data; United Nations Population Division; UNDP; IMF World Economic Outlook Database  
Note: Figures are for total People's Republic of China

**Table 10: Key coping capacity indicators**

Financial inclusion (% of population aged 15+ with access to bank account)	Female pop: 58%
Insurance coverage	1.24% (2019)
Share of population covered by public safety nets	N/A
Internet coverage (% of population using the internet)	54 (2017)
Metabiota Epidemic Preparedness Index	63 (2019)
(100 = maximum score, 0 = minimum score)	78 (2019)
Public and private health expenditure (% of GDP)	5.15 (2017)
Number of physicians (per 1,000)	2 (2017)
Number of hospital beds (per 1,000)	4.2 (2012)
Government effectiveness (-2.5 to +2.5)	0.52 (2019)
Corruption Perception Index	41 (2019)

The potential for resilience to natural hazard risks largely depends on three factors: the country's adaptive capacity, including the effectiveness of government services, such as education and health system; the availability of a communication and early warning system; and the availability of financial resources to prepare and respond. Table 9 shows key coping capacity indicators.

## Disaster risk finance

Disaster risk financing responsibilities in the PRC are shared between national and provincial government. The national government is responsible for Level I (extraordinarily severe disasters); the local and national governments cover Level II (major disasters) and Level III (larger disasters); and local governments handle Level IV (ordinary disasters).

At the provincial level, under the 1994 Budget Law, local governments are expected to save 1-3% of their annual expenditures for unexpected events, including natural disasters. However, both the IMAR and XUAR regions rely heavily on central transfer payments and, incorporating the impacts of local government financing vehicles. In 2019, IMAR's general budgetary revenue, composed of tax and non-tax revenues, was equal to only 40% of total budgetary expenditure. In XUAR, in 2019, the equivalent figure was 30%. The remaining shortfall was met by transfers from central government and the issuance of debt, although the precise balance is unclear.<sup>21</sup>

At the national level, reconstruction funding is determined by the Ministry of Finance and approved by the State Council. In addition, the Central Natural Disaster Livelihood Subsidy Fund aims to support the livelihoods of those affected by disaster events. To help improve its ability to cover the costs associated with disaster events, the state-owned reinsurer China Re issued its first catastrophe bond, for \$50 million of earthquake risk, in 2015.<sup>22</sup> The national government also benefits from a strong fiscal position with an investment grade credit rating.



<sup>21</sup> National Bureau of Statistics (2020), IMAR. Available at: <http://data.stats.gov.cn/search.htm?s=内蒙古财政收入>  
National Bureau of Statistics (2020), XUAR. Available at: <http://data.stats.gov.cn/search.htm?s=新疆财政收入>

<sup>22</sup> <https://www.artemis.bm/news/panda-re-ltd-2015-1-the-first-cat-bond-covering-chinese-perils/>



Protection Gap

The protection gap is traditionally defined as the proportion of losses from disaster events that are not insured. Identifying the level of risk which has not been reduced (through risk reduction investment) or transferred (through risk financing) is to identify

the contingent liability that will need to be met in the event of a disaster. This is important for the design of risk management and arrangement of risk financing: identifying the protection gap informs on where financing is most needed. Table 11 provides the details underpinning this assessment for IMAR and Table 12 provides similar details for XUAR.

Table 11: Key Protection Gap indicators – IMAR

AAL as % of GDP <sup>3</sup>	0.09%	
Un-funded AAL, (\$m, %)	N/A	
Average annual human losses from flood and earthquakes	Flood	EQ
	8	40
Event frequency where direct & indirect loss and damage, less (assumed) insured losses, exceed existing ex-ante risk retention	Flood	EQ
	N/A	N/A
Event frequency where direct damage, less (assumed) insured losses, exceed existing ex-ante risk retention	Flood	EQ
	N/A	N/A
Event frequency where estimated emergency response costs exceed current risk retention mechanisms	Flood	EQ
	N/A	N/A
Macro-economic context and ability for sovereign to borrow	Unclear but potentially weak at the autonomous regions level. Robust national financing arrangements.	
Ability of individual and households to access resources after an event	Statistics not comparable to rest of CAREC but likely to be moderate-high.	

Table 12: Key Protection Gap indicators – XUAR

AAL as % of GDP <sup>23</sup>	0.12%	
Un-funded AAL, (\$m, %)	N/A	
Average annual human losses from flood and earthquakes	Flood	EQ
	5	84
Event frequency where direct & indirect loss and damage, less (assumed) insured losses, exceed existing ex-ante risk retention	Flood	EQ
	N/A	N/A
Event frequency where direct damage, less (assumed) insured losses, exceed existing ex-ante risk retention	Flood	EQ
	N/A	N/A
Event frequency where estimated emergency response costs exceed current risk retention mechanisms	Flood	EQ
	N/A	N/A
Macro-economic context and ability for sovereign to borrow	Unclear but potentially weak at the autonomous regions level. Robust national financing arrangements.	
Ability of individual and households to access resources after an event	Statistics not comparable to rest of CAREC but likely to be moderate-high.	

Source: Consultant team modelling

<sup>23</sup>losses are expressed relative to GDP in the region in 2019 international dollars, as GNI data at the provincial level in the PRC is not available

Both flood and earthquake risk are significant in IMAR. Direct AAL from the two perils in combination are equivalent to around \$369 million or 0.09% of GDP. In XUAR, both absolute and proportionate losses are somewhat greater: \$390 million and 0.12% of GDP excluding indirect losses, and \$442 million and 0.14% including indirect losses.

Insurance penetration in IMAR is high: non-life insurance penetration is 1.24% and insurance density is \$126. These high figures are driven by what the compulsory crop insurance through the China Agricultural Policy Insurance Program (CAPIP). In 2012, 95% of farms in IMAR were insured through this Program, while livestock insurance is also compulsory.<sup>24</sup> By contrast, buildings insurance for flood and earthquake risk is less extensive.

Insurance penetration in XUAR is also high—non-life insurance penetration of 1.66% and insurance density of \$128—driven largely by agricultural insurance through the CAPIP.

It is difficult to assess the protection gap specifically for IMAR and XUAR that is comparable to that of the sovereign countries elsewhere in the CAREC region. On one hand, the level of risk is relatively high, property insurance penetration is limited, and the ability of the provincial governments, acting unilaterally, to quickly and easily finance contingent liabilities through new debt issuance may be difficult. On the other hand, both regions are able to make use both of the explicit ex-ante disaster risk financing measures of the central government, as well as its extensive ability to arrange financing ex-post.

<sup>24</sup> Zhao, Y., Chai, Z., Delgado, M. and Preckel, P. (2016) An empirical analysis of the effect of crop insurance on farmers' income: Results from Inner Mongolia in China. China Agricultural Economic Review 8(2): 299-313

